arXiv:1304.5012v2 [cond-mat.mes-hall] 23 Apr 2013

Inter-surface interaction via phonon in three-dimensional topological insulator

Tetsuro Habe
Department of Applied Physics, Hokkaido University, Sapporo 060-8628, Japan

(Dated: April 24, 2013)

In topological insulators, the phonon plays the important role in electron-electron interaction. We consider the surface electric state on the three-dimensional topological insulator with inter-surface interaction via phonon theoretically. In this work, we derive the effective two-dimensional model in which two surface states of the topological insulator are coupled by the Fermi interaction. In the resultant model, the sign of the coupling constant changes depending on the temperature and the ratio of the speeds for the phonon and the surface state of the topological insulator. As a consequence, we show the prescription to tune the sign and the magnitude of the inter-surface interaction via phonon in a three-dimensional topological insulator.

I. INTRODUCTION

The three-dimensional(3D) topological insulator(TI) has two-dimensional(2D) massless electric states on its surface[1–4]. The massless surface state is represented by a Dirac Hamiltonian in high-energy physics and has a linear energy dispersion so called as a Dirac cone topologically protected. Theoretically, without the interactions, a mass term dose not appear unless the system looses time reversal symmetry(TRS)[5–11]. On the other hand, with the interactions, there is a well known dynamical mass generation for the massless fermion represented by the Dirac Hamiltonian in association with the spontaneously symmetry breaking (SSB) of chiral $U(1)$ symmetry[12,13]. The dynamical mass appears when two Dirac cones are coupled attractively. In a 3D TI, the inter-surface interaction plays a important role in the dynamical mass generation because there is a single Dirac cone at one surface of the TI. Thus it is important to study the sign of the coupling constant for the inter-surface interaction.

The TIs with the inter-surface interaction via electromagnetic field have been studied theoretically in the sample of a thin film[14–20]. Since the Coulomb interaction is always repulsive, the large gate voltage, i.e.the difference of Fermi energies for two surfaces, is necessary for SSB. However, the interaction via phonon is more responsible in TIs than the Coulomb interaction because the Coulomb interaction is suppressed in TIs with a much larger dielectric constant than that in the vacuum. The effects of the electron-electron interaction via phonon have been one of the hot issues in the study of 3D TIs[21–27]. However, the effects of the inter-surfaces interaction via phonon between two surfaces are lacked in the study of phonon in a TI.

In this paper, we discuss the TI with the inter-surface interaction via phonon and the condition for the inter-surface interaction to be attractive. We construct a simple 2D model from the two surfaces interacting via phonon in a 3D TI and calculate the coupling constant with perturbation expansion. As a result, we find the inter-surface interaction via the phonon change to be attractive if the phonon speed comes close to the Fermi speed of the surface state.

This paper is organized as follows. In Sec. II, we explain our theoretical model. The inter-surface interaction is calculated numerically in Sec. III. The conclusion is given in Sec. IV.

II. THEORETICAL MODEL

We consider two pseudo (2+1)-dimensional surface states which are staying at the opposite surface of a 3D TI shown in Fig. 1. The surface state is constructed of a two-dimensional wave component $\psi = (\xi, \eta)$ and a wave component damping in the bulk of the TI. We assume that the penetration length λ is a constant value for each surface states and that the surface state Ψ is represented

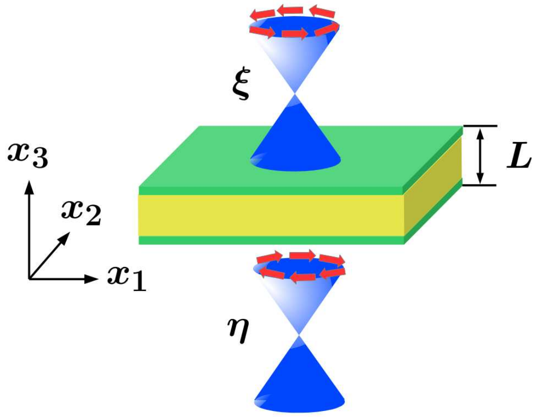

FIG. 1. The schematic of two surface states is shown. The ξ and η which are two-dimensional component of the surface states in the plane sample of TI. Two cones represent the energy dispersions of the surface states. The arrows on the cones show the direction of spin direction locked by the momentum.

in three-dimension by,

$$\Psi = \begin{pmatrix} f_+(x_3) & 0 \\ 0 & f_-(x_3) \end{pmatrix} \psi \tag{1}$$

$$f_\pm(x_3) = \frac{1}{\sqrt{\lambda}} \exp\left[\ \mp \frac{1}{2\lambda}\left(x_3 \pm \frac{L}{2} \right) \ \right] \tag{2}$$

$$\psi = \begin{pmatrix} \xi(t, x_1 x_2) \\ \eta(t, x_1 x_2) \end{pmatrix}, \tag{3}$$

where ξ and η are the two-dimensional wave components of two-surface states shown in Fig. 1. In the vicinity of the Dirac point in two-dimensional momentum space parallel to the surface, the Lagrangian of the surface state is represented as Weyl field by using a notation of $\bar{\Psi} = \Psi^\dagger \gamma^0$,

$$\mathscr{L}_e = -i\bar{\Psi}\gamma^\mu \tilde{\partial}_\mu \Psi \tag{4}$$

where the index which appears twice in a single term means the summation for $\mu = 0, 1, 2$, γ^μ is Dirac gamma matrices for $\mu = 0-3$,and 5, $\tilde{\partial}_\mu$ represents the derivative for time $\partial_0 = \tilde{\partial}_0 = \partial/\partial t$ and in-plane axis $\tilde{\partial}_j = v_F \partial_j = v_F \partial/\partial x_j$ for $j = 1$ and 2 with the Fermi velocity v_F. Two surface states ξ and η are separated in x_3-axis of a distance L. We consider a thick enough TI so that $\lambda/L \ll 1$ is satisfied and ignore a direct hopping between the surface states. Thus the coupling between the surface states is dominated by a phonon field.

A. Effective 2D Lagrangian of electron-phonon coupling

Let us derive a 2D effective electron-phonon interaction Lagrangian from three-dimensional model where the two surface states are interacting by the three-dimensional phonon. In the bulk of the TI, we assume the electron-phonon interaction can be ignored when the Fermi energy lies in bulk gap of the TI. The Lagrangian density of the phonon can be represented by use of the scalar boson field ϕ and it is the Klein-Gordon Lagrangian density as,

$$\mathscr{L}_p = (\partial_0 \Phi)^2 - \sum_{j=1-3} (v_B \partial_j \Phi)^2 - \frac{m^2}{2}\Phi^2, \tag{5}$$

where v_B and m are the speed and the mass of boson respectively. The mass appears for an optical phonon or an acoustical phonon under the pressure[21]. The free boson has the eigen energy $\omega_k = \sqrt{v_B{}^2 |\boldsymbol{k}|^2 + m^2}$ with the momentum $\boldsymbol{k}$. In the point of view for a lattice vibration, the displacement vector $\boldsymbol{u}$ is obtained by the boson field e.g., $\boldsymbol{u} = \boldsymbol{\nabla}\phi$ for an acoustical phonon. The scalar field Φ can be represented by a product of the wave component along x_3-axis and the in-plane wave component of $\phi(t, x_1, x_2, k_3)$ as

$$\Phi(t, x) = \int \frac{dk_3}{\sqrt{2\pi}} \phi(t, x_1, x_2, k_3) \frac{1}{\sqrt{2\pi}} \sin k_3 x_3, \tag{6}$$

under the Dirichlet boundary condition of $\Phi(t, x) = 0$ at $x_3 = 0$. We discuss the coupling between the Weyl field and the phonon field in the coordinate system with the boundary at $x_3 = 0$.

The Lagrangian of the interaction contains the overlap between the wave functions of the Weyl field and the phonon field along x_3-axis.

$$\begin{aligned} L_{ep} = \int d^3\boldsymbol{x} U \left\{ \xi^\dagger(x)\xi(x) f_+{}^2(x_3) \right. \\ \left. + \eta^\dagger(x)\eta(x) f_-{}^2(x_3) \right\} \Phi, \end{aligned} \tag{7}$$

where the integral is defined in (x_1, x_2, x_3) and $\zeta(x) = \zeta(t, x_1, x_2)$ for $\zeta = \xi$ and η. In the following, we omit the valuable x in the integrand when the valuable coincides with the integral valuable for convenience. The overlap of the wave functions of the Weyl field and the phonon field along x_3-axis can be calculated as

$$\begin{aligned} \chi =& \frac{1}{2\pi\lambda} \int_0^L dx_3 \sin k_3 x_3 \exp\left[-\frac{x_3}{\lambda} \right] \\ =& \frac{1}{2\pi} \frac{1}{1 + (k_3\lambda)^2} \left(e^{-\frac{L}{\lambda}} [\sin k_3 L - k_3 \lambda \cos k_3 L] + k_3 \lambda \right) \\ \simeq& \frac{k_3 \lambda}{2\pi}, \end{aligned} \tag{8}$$

under the limit of a small penetration length λ as $L/\lambda \to \infty$ and $1 + k_3\lambda \to 1$. The interaction Lagrangian L_{ep} is represented by

$$L_{ep} = \int dx_1 dx_2 \ \tilde{\phi}\{\xi^\dagger \xi + \eta^\dagger \eta\}, \tag{9}$$

$$\tilde{\phi}(t, x_1, x_2) = \int dk_3 \chi(k_3) U(k_3) \phi(t, x_1, x_2, k_3). \tag{10}$$

We obtain the effective Lagrangian in 2D space (x_1, x_2). In the following, the integral is defined in $x = (t, x_1, x_2)$ as $d^3x \equiv dt dx_1 dx_2$.

B. Inter-surface interaction of Weyl field

In this paper, we focus on representing the inter-surface interaction as

$$V = -g \ \xi^\dagger \xi(x) \ \eta^\dagger \eta(x), \tag{11}$$

without the explicit phonon momentum and energy. As a starting point, we consider the Lagrangian of the inter-surface interaction intermediated by a phonon represented by

$$\mathscr{L}_{\rm int} = -\int dk_3 u^2 \xi^\dagger \xi(x) D(x - x') \zeta^\dagger \zeta(x'), \tag{12}$$

with $u = \chi U$ and a phonon propagator $D(x - x')$ (see Appendix A). The Lagrangian of interaction can be interpreted easily as the exchanging the phonon and shown as a Feynman diagram in Fig. 2-(b).

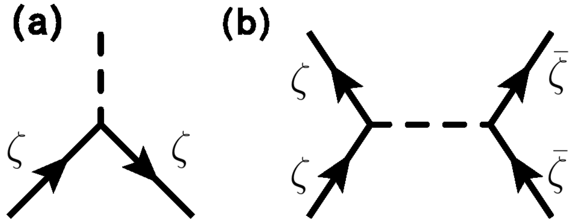

FIG. 2. The Feynman diagrams of (a) the vertex function in Eq.(7) and (b) the lowest order term for electron-electron interaction via the phonon exchanging are shown. The label ζ denotes the surface Weyl field for $\zeta = \xi,\ \eta$. In Fig. (b), ζ and $\bar\zeta$ represent opposite surface field operator, *i.e.* $(\zeta, \bar\zeta) = (\xi, \eta)$ or $(\zeta, \bar\zeta) = (\eta, \xi)$. This diagram represent the first-order effective inter-surface interaction through a phonon.

Generally, the effective action Γ is summation of the Lagrangian in Eq. (4), (12) and one-particle irreducible(1PI) vertex functions $\kappa^{[1\mathrm{PI}]}$ which contains the loop diagrams

$$\Gamma = \int d^3x \left(\mathscr{L}_e + \mathscr{L}_{\mathrm{int}} + \kappa^{[1\mathrm{PI}]} \right). \tag{13}$$

In this paper, we employ the effective potential instead of the one-loop 1PI vertex function shown in Fig. 3. The effective potential is

$$V = -\mathscr{L}_{\mathrm{int}} - \kappa^{[1\mathrm{PI}]} \tag{14}$$

under the condition in which the initial sate and the final state have a same energy and momentum i.e., we assume the coupling constant of interaction between any states ξ and η in momentum space to be a single coupling constant g as

$$V = -g\xi(p_1)\xi(p_1 + p')\eta(p_2)\eta(p_2 - p') \tag{15}$$

where $p = (p_0, \boldsymbol{p})$ are the energy p_0 and the momentum $\boldsymbol{p}$. The coupling constant g is calculated with $p' = 0$. The assumption is applicable in low energy theory when the interaction contains no divergent term in the infrared region. The effective potential in Eq. (15) is transformed to the inter-surface coupling in Eq. (11) by Fourier transformation.

To calculate the effective potential, we introduce the propagators of the Weyl field and those of the phonon in order to calculate the effective potential in momentum space. The propagator of the Weyl field $G(p_0, \boldsymbol{p})$ and the phonon $D(k_0, \boldsymbol{k})$ in energy-momentum space are represented by

$$G(p_0, \boldsymbol{p}) = \frac{1}{p_0\sigma^0 - v\boldsymbol{p}\cdot\boldsymbol{\sigma} + i\epsilon}, \tag{16}$$

$$D(p_0, \boldsymbol{p}) = \frac{2\sqrt{v_B{}^2\boldsymbol{p}^2 + \tilde{m}^2}}{p_0{}^2 - v_B{}^2\boldsymbol{p}^2 - (\tilde{m}^2 - i\epsilon)}, \tag{17}$$

$$\tilde{m} = m + v_B{}^2 k_3{}^2 \tag{18}$$

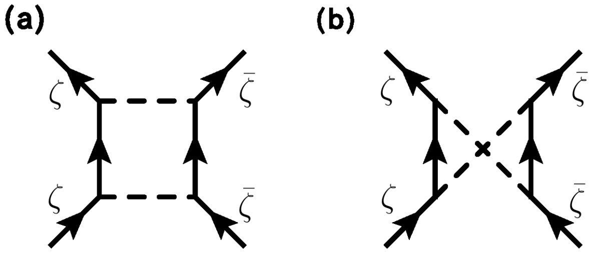

FIG. 3. The Feynman diagrams of the second order inter-surface interaction are shown.

where σ^ν is 2×2 unit matrix for $\nu = 0$, Pauli matrices for $\nu = 1 - 3$, p_0 and $\boldsymbol{p} = (p_1, p_2)$ are energy and two-dimensional momentum.

In this work, we consider two types of coupling between a phonon and an electron, the deformation and polar coupling[28]. Another type of coupling called as the piezoelectric coupling is suppressed by inversion symmetry of the materials[22,29] and, ignored in this paper. The two couplings are represented by the different vertex functions $M_p^{(D)}$ and $M_p^{(P)}$ which are the Fourier component of u as

$$\left(M_p^{(D)}\right)^2 = C_1\chi^2 \frac{v_F|\boldsymbol{p}|^2}{p_D} \tag{19}$$

$$\left(M_p^{(P)}\right)^2 = C_2\chi^2 \sqrt{v_B{}^2|\boldsymbol{p}|^2 + \tilde{m}^2}, \tag{20}$$

where C_1 and C_2 are the coupling constants and the superscripts (D) and (P) denote the deformation and polar couplings respectively. The coupling constants are represented by

$$C_1 = \frac{p_D}{v_F} R^2 \tag{21}$$

$$C_2 = 2\pi e^2 \left(\frac{1}{\varepsilon_\infty} - \frac{1}{\varepsilon} \right) \tag{22}$$

where R is the deformation constant, p_D is a Debye momentum and ε_∞, and ε are the dielectric constants for a high-frequency and a low-frequency, respectively[28]. We consider both couplings in this work because it is unclear which coupling is more dominant in TIs. The deformation coupling is responsible for the interaction between the electron and the acoustical phonon. On the other hand, the polar coupling accounts for the interaction between the electron and the optical phonon. The some experiments suggest that the optical phonon play a dominant role[30,31], however the other experiment[32] and the theory of the acoustical phonon[22]have a good agreement in the life-time of a quasi-particle in the surface of TIs.

C. Deformation coupling

At first, we consider the deformation coupling. In no-loop calculation, the deformation coupling is vanished as

$$\begin{aligned} \mathscr{L}_{\text{int}} =& g^{(0)} \xi^\dagger \xi(p) \zeta^\dagger \zeta(-p) & (23) \\ g^{(0)} =& -\lim_{p_\mu \to 0} \int dk_3 {M_p^{(D)}}^2 D(p_0, \boldsymbol{p}) = 0, & (24) \end{aligned}$$

where the superscript of $g^{(0)}$ denotes the number of loops.

Thus we must consider the one-loop effective potential $V_a^{(1)}$ and $V_b^{(1)}$ in which the subscript denotes two labels in Fig. 3. The one-loop effective potentials are represented by

$$\begin{aligned} V_a^{(1)} =& \int dk_3 \int \frac{d^3p}{(\sqrt{2\pi})^3} {M_p^{(D)}}^4 \left(\xi^\dagger G(p_0, \boldsymbol{p}) \xi\right) \\ & \times \left(\eta^\dagger G(-p_0, -\boldsymbol{p}) \eta\right) D(p_0, \boldsymbol{p})^2 & (25) \\ V_b^{(1)} =& \int dk_3 \int \frac{d^3p}{(\sqrt{2\pi})^3} {M_p^{(D)}}^4 \left(\xi^\dagger G(p_0, \boldsymbol{p}) \xi\right) \\ & \times \left(\eta^\dagger G(p_0, \boldsymbol{p}) \eta\right) D(p_0, \boldsymbol{p})^2, & (26) \end{aligned}$$

where ξ and η are independent of $(p_0, \boldsymbol{p})$. The whole effective potential can be represented by

$$\begin{aligned} V^{(1)} = \int dk_3 \int \frac{d^3p}{(\sqrt{2\pi})^3} {M_p^{(D)}}^4 (& \, {p_0}^2 \Gamma_1(p) \xi^\dagger \xi \; \eta^\dagger \eta \\ & + {p_i}^2 \Gamma_2(p) \xi^\dagger \sigma^i \xi \; \eta^\dagger \sigma^i \eta \,), \quad (27) \end{aligned}$$

where the terms with a odd number of momentums p_i are ignored here because they will be vanished at the momentum integration. Using the Matsubara method, we can calculate the effective potential in a finite temperature $T = \beta^{-1}$ as

$$V^{(1)} = -g^{(1)} \xi^\dagger \xi \; \eta^\dagger \eta, \tag{28}$$

where the second term in Eq. (27) is cancelled out. The effective coupling constant $g^{(1)}$ is

$$\begin{aligned} g^{(1)} =& \frac{1}{2} \int dk_3 \int dp \; p(\omega_p (M_p^{(D)})^2)^2 \Gamma_1(p) & (29) \\ \Gamma_1(p) =& \Gamma_{FB}(p) + \Gamma_F(p) + \Gamma_B(p) \\ \Gamma_{FB}(p) =& \beta[\tilde{D}_A(p)^2 + \tilde{D}_R(p)^2] \\ & \times [n_F(\varepsilon_p) n_F(-\varepsilon_p) + n_B(\omega_p) n_B(-\omega_p)] & (30) \\ \Gamma_F(p) =& -\frac{1}{\varepsilon_p} \Big([1 - 4{\varepsilon_p}^2 \tilde{D}_A(p)] \tilde{D}_A(p)^2 n_F(\varepsilon_p) \\ & -[1 - 4{\varepsilon_p}^2 \tilde{D}_R(p)] \tilde{D}_R(p)^2 n_F(-\varepsilon_p) \Big) & (31) \\ \Gamma_B(p) =& \frac{1}{\omega_p} \Big([1 + 4{\omega_p}^2 \tilde{D}_A(p)] \tilde{D}_A(p)^2 n_B(\omega_p) \\ & -[1 + 4{\omega_p}^2 \tilde{D}_R(p)] \tilde{D}_R(p)^2 n_B(-\omega_p) \Big) & (32) \end{aligned}$$

where $\omega_p = \sqrt{{v_B}^2 |\boldsymbol{p}|^2 + \tilde{m}^2}$ and $\varepsilon_p = v_F |\boldsymbol{p}|$ are the energies of phonon and surface Weyl field respectively. The integral range of momentum is $0 < \sqrt{p^2 + {k_3}^2} < p_D$ with a Debye momentum p_D. The Bose and Fermi distribution functions $n_B(z)$ and $n_F(z)$ are represented by

$$\begin{aligned} n_B(z) =& \frac{1}{e^{\beta z} - 1} & (33) \\ n_F(z) =& \frac{1}{e^{\beta z} + 1}. & (34) \end{aligned}$$

The propagator $\tilde{D}_{A(R)}(p)$ is defined as

$$\tilde{D}_{A(R)}(p) = \frac{1}{{\omega_p}^2 - {\varepsilon_p}^2 - (+) i\epsilon}. \tag{35}$$

We calculate $g^{(1)}$ with an unit of $\varepsilon_{\text{def}} = {C_1}^2 p_D / v_F$ numerically by changing three parameters β, $\gamma = v_B/v_F$ and m under the normalization by the Debye momentum p_D and the energy $\omega_D = \sqrt{m^2 + {v_B}^2 {p_D}^2}$ in Fig. 4. In the materials of TIs, γ takes a small value of 10^{-2} approximately i.e., the phonon speed is much smaller than the surface fermion speed $v_B \ll v_F$. For small γ, the phonon contributes to the repulsive inter-surface interaction shown in Fig. 4-(a). Increasing the speed ratio γ, however, the region of the repulsive inter-surface interaction is decreasing in Fig. 4-(b). Eventually, the attractive inter-surface interaction becomes dominant under any mass m and temperature β^{-1} in Fig. 4-(c).

D. Polar coupling

Next, we consider the polar coupling and obtain the finite attractive interaction in the no-loop calculation as

$$\begin{aligned} g^{(0)} =& \lim_{p_\mu \to 0} \int dk_3 {M_p^{(P)}}^2 D(p_0, \boldsymbol{p}) = 2 C_2 \kappa, & (36) \\ \kappa =& \frac{\lambda^2}{8{v_B}^3} \left(v_B p_D \omega_D (2{\omega_D}^2 - m^2) - m^4 \ln \frac{v_B p_D + \omega_D}{m} \right), \end{aligned}$$

where κ is always positive value. The no-loop term of the phonon has opposite sign to that of the photon(see Appendix B). We also calculate the one-loop correction $g^{(1)}$ with an unit of $\varepsilon_{\text{pol}} = {C_2}^2 p_D / v_F$ in this coupling shown in Fig. 5. For the polar coupling, the crossover between a repulsive coupling constant and a attractive coupling constant occurs at a lower γ than the deformation coupling.

We should point out that it is difficult to decide which interaction via deformation or polar coupling is more dominant because the coupling constants C_i in Eq. (19) and (20) are unknown in TIs. However, these results with two couplings show that there is the attractive inter-surface interaction when the system has the slow Dirac mode or the fast phonon mode i.e., the speed ratio γ is larger than the ordinary 3D TIs of Bi_2Se_3, Bi_2Te_3 and Sb_2Te_3. In Figure 6, the coupling constant $g^{(1)}$ is shown as a function of γ and the temperature $T = \beta^{-1}$. The coupling constant $g^{(1)}$ must become attractive if the speed ratio γ is larger than 0.25.

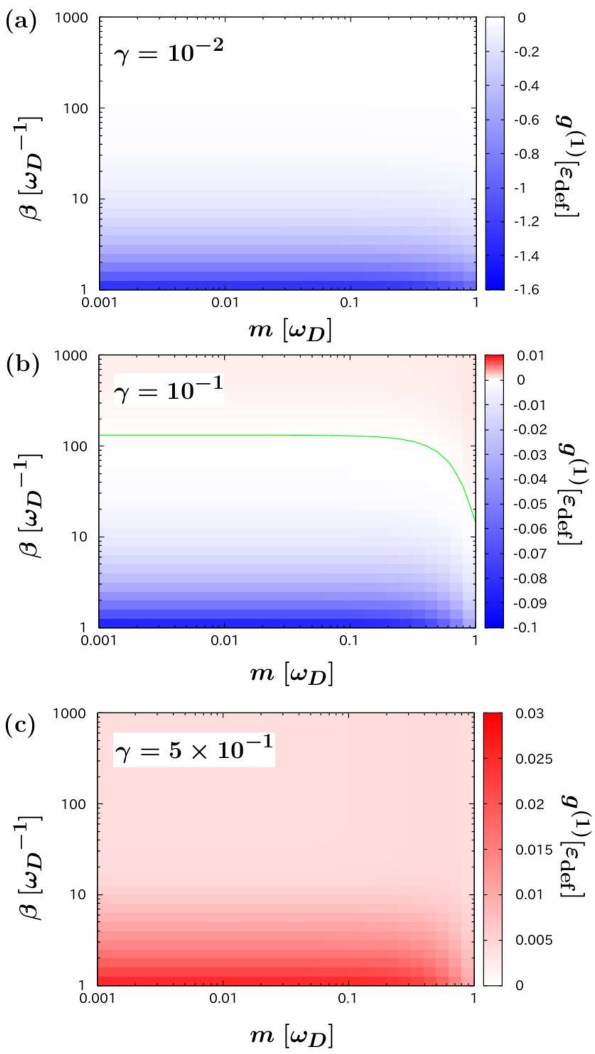

FIG. 4. The coupling constant $g^{(1)}$ with an unit of $\varepsilon_{\rm def} = {C_1}^2 p_D/v_F$ of the inter-surface interaction via deformation in Eq. 28 are shown. The potential becomes attractive in red region and repulsive in the blue region and the zero-potential is represented by the green line.

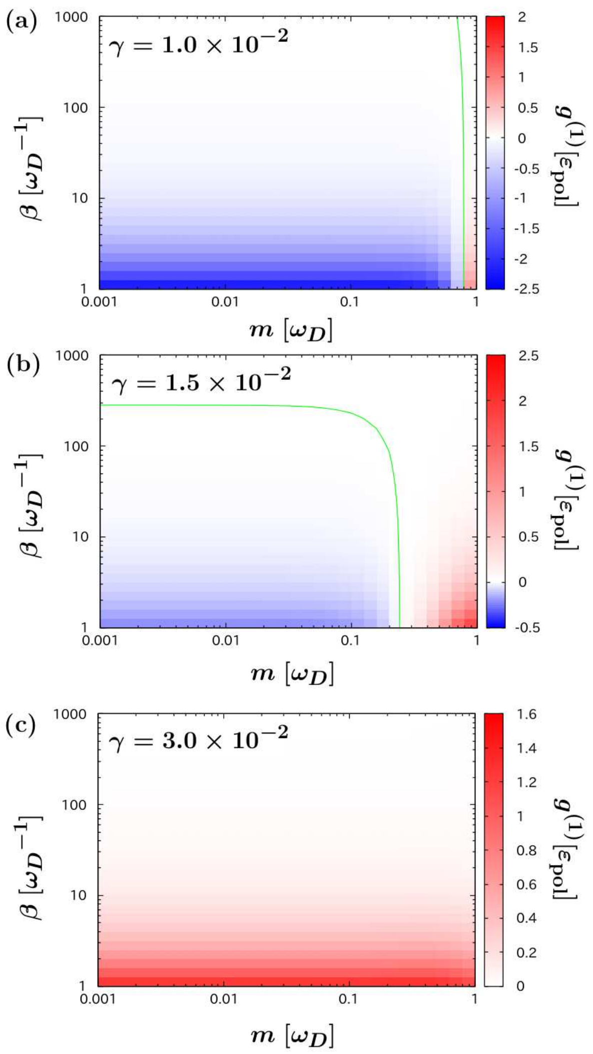

FIG. 5. The coupling constant $g^{(1)}$ with an unit of $\varepsilon_{\rm pol} = {C_2}^2 p_D/v_F$ of the inter-surface interaction via the polar coupling in Eq. 28 are shown. The potential becomes attractive in red region and repulsive in the blue region and the zero-potential is represented by the green line.

At the end of this section, we show the resultant Lagrangian density describing the opposite surface is represented by

$$\mathscr{L} = -i\bar{\psi}\gamma^\mu\tilde{\partial}_\mu\psi(x) + g(\bar{\psi}\psi(x) + \bar{\psi}\gamma^5\psi(x)). \tag{37}$$

This model is purely two-dimensional $x = (t, x_1, x_2)$ and the interaction is a summation as $g = g^{(0)} + g^{(1)}$. The model Lagrangian density is so called as the Nambu-Jona Lasino model which represent a dynamical mass generation for a large positive g in association with the spontaneously symmetry breaking of chiral $U(1)$ symmetry breaking[12,13]. We have shown that g becomes positive with a larger γ than ordinal TIs. Therefore, the intrinsic dynamical mass generation via a phonon is possible to be appeared in the TI when the TI has a slow Dirac mode on its surface or a fast phonon mode in the bulk of TI.

III. CONCLUSION

We consider the inter-surface interaction via the phonon which propagates in the bulk of 3D TI. When the phonon speed is much smaller than the Fermi speed of the surface Dirac particle, the phonon result in a repulsive inter-surface interaction. On the other hand, when the phonon speed catch up to the Fermi speed, the all phonon modes enhance an attractive inter-surface interaction. The resultant effective Lagrangian can be represented by the Nambu-Jona Lasino model with a attractive interaction.

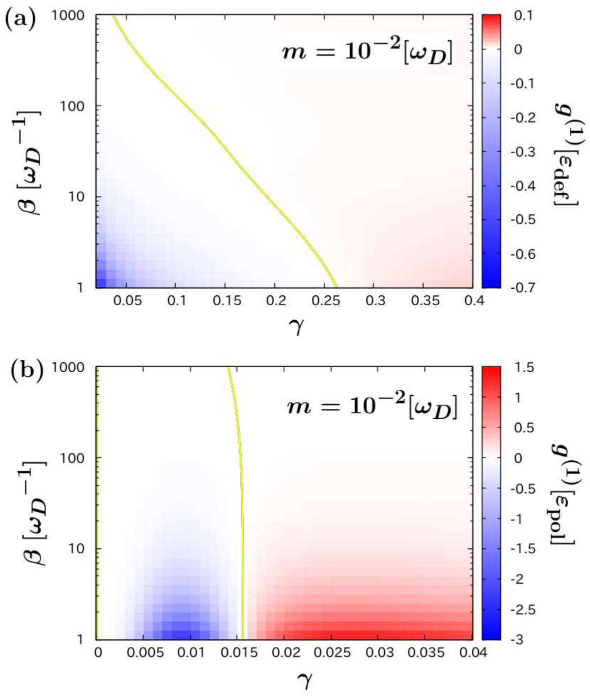

FIG. 6. The coupling constant of the inter-surface interaction via the polar coupling in Eq. 28 are shown. These figures calculated by use of (a) deformation and (b) polar coupling with $m = 10^{-3}[\omega_D]$. The potential becomes attractive in red region and repulsive in the blue region, and the zero-potential is represented by the green line.

ACKNOWLEDGMENTS

I would like to thank Yasuhiro Asano for helpful conversation and comments.

Appendix A: Effective action of Weyl field

In this section, we derive the effective inter-surface interaction like Eq. (12) from the Lagrangian of Eq. (5) and (9) by the path-integral method. The effective action Γ which contains the effective interaction is acquired from the generating functional of a propagator Z represented by,

$$Z[z,\bar{z},J] = \int \mathscr{D}\psi\mathscr{D}\bar{\psi}\mathscr{D}\phi \exp i \int d^3x \mathscr{L} \tag{A1}$$

$$\mathscr{L} = \mathscr{L}_e + \mathscr{L}_p + u_0(\bar{\psi}\gamma_0\psi)\phi + J\phi + \bar{z}\psi + z\bar{\psi}, \tag{A2}$$

where $z(x)$, $\bar{z}(x)$ and $J(x)$ are the virtual external sources and we introduce the coupling constant u_0. The effective action is the generating functional of the vertex function[33]. To omit an explicit phonon field, we consider that there is no phonon source as $J = 0$ and calculate the path-integral for ϕ,

$$\begin{aligned} Z[z,\bar{z}] &= \int \mathscr{D}\psi\mathscr{D}\bar{\psi} \exp\left[i\int d^3x \mathscr{L}'_e\right] Z_0[j(x)], \qquad (A3)\\ \mathscr{L}'_e &= \mathscr{L}_e + \bar{z}\psi + z\bar{\psi},\\ Z_0[j(x)] &= \exp\left[-i\int d^3x \int d^3x' j(x)D(x-x')j(x')\right],\\ j(x) &= u(\bar{\psi}\gamma_0\psi)(x), \end{aligned}$$

with the phonon propagator $D(x)$. The calculation is same as the case of a non-interacting scalar boson with external source of $j(x)$ and provides the generating functional of phonon propagator as $Z_0[j(x)]$. We obtain the four point term in Z_0 which represents an effective interaction in Weyl field,

$$\mathscr{L}_{\rm int} = -j(x)D(x-x')j(x'). \tag{A4}$$

The interaction can be interpreted easily as the exchanging the phonon. The Lagrangian contains an intra-surface interaction proportional to the fourth-order term of ξ or η in Eq. (11) and an inter-surface interaction which consist of the product of the quadratic term of ξ and the quadratic term of η. The effective action can be derived as a summation of one-particle irreducible vertex functions which consist of four-field potential in Eq. (A4).

Appendix B: The Coulomb interaction

The interaction Lagrangian via a photon in Feynman gauge is represented by

$$\mathscr{L}_{\rm int} = -e^2\bar{\psi}\gamma^{\mu}\psi D_{\mu\nu}(p)\bar{\psi}\gamma^{\nu}\psi \tag{B1}$$

$$D_{\mu\nu}(p) = \frac{-g_{\mu\nu}}{{p_0}^2 - |\boldsymbol{p}|^2 + i\varepsilon}, \tag{B2}$$

where the speed of light is unity $c = 1$ and $g_{\mu\nu}$ is the metric tensor as,

$$g_{\mu\nu} = {\rm diag}[1,-1,-1,-1], \tag{B3}$$

with $\mu,\ \nu = 0 - 3$. Using the longitudinal component given by $D_{00}(p)$, the interaction without energy transfer $p_0 = 0$ can be represented by

$$\mathscr{L}_{\rm int} = -(\xi^{\dagger}\xi + \eta^{\dagger}\eta)\frac{e^2}{|\boldsymbol{p}|^2}(\xi^{\dagger}\xi + \eta^{\dagger}\eta) \tag{B4}$$

$$= -\frac{e^2}{|\boldsymbol{p}|^2}\left(\sum_{\zeta=\xi,\eta}\zeta^{\dagger}\zeta\zeta^{\dagger}\zeta + 2\xi^{\dagger}\xi\eta^{\dagger}\eta\right). \tag{B5}$$

It is obviously for the first and second terms are the intra-surface and inter-surface Coulomb interactions respectively. This interaction is repulsive in contrast to the phonon in Eq. (36) because the photon propagator in Eq. (B2) is opposite sign to the phonon propagator in Eq. (17).

---

[1] L. Fu, C. L. Kane, and E. J. Mele, Phys. Rev. Lett. **98**, 106803 (2007).

[2] L. Fu and C. L. Kane, Phys. Rev. B. **76**, 045302 (2007).

[3] J. E. Moore and L. Balents, Phys. Rev. B. **75**, 121306 (2007).

[4] Y. L. Chen, J. G. Analytis, J.-H. Chu, Z. K. Liu, S. K. Mo, X. L. Qi, H. J. Zhang, D. H. Lu, X. Dai, Z. Fang, S. C. Zhang, I. R. Fisher, Z. Hussain, and Z. X. Shen, Science **325**, 178 (2009).

[5] Y. Tanaka, T. Yokoyama, and N. Nagaosa, Phys. Rev. Lett. **103**, 107002 (2009).

[6] D. Hsieh, Y. Xia, D. Qian, L. Wray, J. H. Dil, F. Meier, J. Osterwalder, L. P. J. G. Checkelsky, N. P. Ong, A. V. Fedorov, H. Lin, A. Bansil, D. Grauer, Y. S. Hor, R. J. Cava, and M. Z. Hasan, Nature **460**, 1101 (2009).

[7] Q. Liu, C.-X. Liu, C. Xu, X.-L. Qi, , and S.-C. Zhang, Phys. Rev. Lett. **102**, 156603 (2009).

[8] Y. S. Hor, P. Roushan, H. Beidenkopf, J. Seo, D. Qu, J. G. Checkelsky, L. A. Wray, D. Hsieh, Y. Xia, S.-Y. Xu, D. Qian, M. Z. Hasan, N. P. Ong, A. Yazdani, and R. J. Cava, Phys. Rev. B. **81**, 195203 (2012).

[9] Y. L. Chen, J.-H. Chu, J. G. Analytis, Z. K. Liu, K. Igarashi, H.-H. Kuo, X. L. Qi, S. K. Mo, R. G. Moore, D. H. Lu, M. Hashimoto, T. Sasagawa, S. C. Zhang, I. R. Fisher, Z. Hussain, and Z. X. Shen, Science **329**, 659 (2010).

[10] L. A. Wray, S.-Y. Xu, Y. Xia, D. Hsieh, A. V. Fedorov, Y. S. Hor, R. J. Cava, A. Bansil, H. Lin, and M. Z. Hasan, Nat. Phys. **7**, 32 (2010).

[11] T. Habe and Y. Asano, Phys. Rev. B. **85**, 195325 (2012).

[12] Y. Nambu and G. Jona-Lasinio, Phys. Rev. **122**, 345 (1961).

[13] Y. Nambu and G. Jona-Lasinio, Phys. Rev. **124**, 246 (1961).

[14] B. Seradjeh, J. E. Moore, and M. Franz, Phys. Rev. Lett. **103**, 066402 (2009).

[15] J. Wang, A. M. DaSilva, C.-Z. Chang, K. He, J. K. Jain, N. Samarth, X.-C. Ma, Q.-K. Xue, and M. H. W. Chan, Phys. Rev. B **83**, 245438 (2011).

[16] M. Liu, C.-Z. Chang, Z. Zhang, Y. Zhang, W. Ruan, K. He, L.-l. Wang, X. Chen, J.-F. Jia, S.-C. Zhang, Q.-K. Xue, X. Ma, and Y. Wang, Phys. Rev. B **83**, 165440 (2011).

[17] G. Y. Cho and J. E. Moore, Phys. Rev. B **84**, 165101 (2011).

[18] E. G. Moon and C. Xu, Eur. Phys. Lett. **97**, 66008 (2012).

[19] I. Sodemann, D. A. Pesin, and A. H. MacDonald, Phys. Rev. B **85**, 195136 (2012).

[20] D. K. Efimkin, Y. E. Lozovik, and A. A. Sokolik, Phys. Rev. B **86**, 115436 (2012).

[21] W. Cheng and S.-F. Ren, Phys. Rev. B **83**, 094301 (2011).

[22] S. Giraud and R. Egger, Phys. Rev. B **83**, 245322 (2011).

[23] Z.-H. Pan, A. V. Fedorov, D. Gardner, Y. S. Lee, S. Chu, and T. Valla, Phys. Rev. Lett. **108**, 187001 (2012).

[24] X. Zhu, L. Santos, R. Sankar, S. Chikara, C. Howard, F. C. Chou, C. Chamon, and M. El-Batanouny, Phys. Rev. Lett. **107**, 186102 (2011).

[25] S. Giraud, A. Kundu, and R. Egger, Phys. Rev. B **85**, 035441 (2012).

[26] X. Zhu, L. Santos, C. Howard, R. Sankar, F. C. Chou, C. Chamon, and M. El-Batanouny, Phys. Rev. Lett. **108**, 185501 (2012).

[27] O. Viyuela, A. Rivas, and M. A. Martin-Delgado, Phys. Rev. B **86**, 155140 (2012).

[28] G. D. Mahan, *Many-Particle Physics THIRD EDITION* (Plenum, New York, 2000).

[29] B.-L. Huang and M. Kaviany, Phys. Rev. B **77**, 125209 (2008).

[30] K. Shahil, M. Hossain, D. Teweldebrhan, and A. Balandin, Appl. Phys. Lett. **96**, 153105 (2010).

[31] J. Qi, X. Chen, W. Yu, P. Cadden-Zimansky, D. Smirnov, N. H. Tolk, I. Miotkowski, H. Cao, Y. Chen, Y. Wu, S. Qiao, and Z. Jiang, Appl. Phys. Lett. **97**, 182102 (2010).

[32] R. C. Hatch, M. Bianchi, D. Guan, S. Bao, J. Mi, B. B. Iversen, L. Nilsson, L. Hornekær, and P. Hofmann, Phys. Rev. B. **83**, 241303 (2011).

[33] J. W. Negele and H. Orland, *QUANTUM MANY-PARTICLE SYSTEMS* (Westview Press, 1998).